

## MICROSTRUCTURE EXAMINATION AND TENSILE PROPERTIES OF Al-20%Mg<sub>2</sub>Si-XZrO<sub>2</sub> HYBRID COMPOSITES

Hamidreza Ghandvar<sup>1</sup>, Tuty Asma Abu Bakar<sup>2,\*</sup> and Mostafa Abbas Jabbar<sup>3</sup>

<sup>1</sup>Department of Chemical and Materials Engineering, New Uzbekistan University,  
Movarounnahr Street 1, Tashkent, Uzbekistan

<sup>2</sup>Faculty of Mechanical Engineering, Universiti Teknologi Malaysia, Johor Bahru 81310,  
Johor, Malaysia

<sup>3</sup>Department of Mechanical Techniques, Al-Nasiriya Technical Institute, Southern Technical  
University, Thi-Qar, Al-Nasiriya 64001, Iraq

\*tuty@utm.my

---

**Abstract.** Due to the unique properties of aluminium hybrid metal matrix composites (Al hybrid MMC) such as physical, mechanical, and tribological properties, these materials recently achieved considerable attention particularly in automotive and aerospace applications. These unique properties are the result of the presence of two or more reinforcement particles in the composite matrix. In the present study, various concentrations of Zirconium oxide (ZrO<sub>2</sub>) particles were introduced to the Al-Mg<sub>2</sub>Si composite via stir casting technique. The influence of various concentrations of ZrO<sub>2</sub> on the structural and tensile properties of the Al-Mg<sub>2</sub>Si composite was examined using Scanning Electron Microscope (SEM) and tensile tests, respectively. The findings showed that the introduction of ZrO<sub>2</sub> to Al-Mg<sub>2</sub>Si decreased the average mean size of primary Mg<sub>2</sub>Si particulates. Adding ZrO<sub>2</sub> particles up to 10 wt.% had a decent distribution in the Al-Mg<sub>2</sub>Si matrix; however, increasing the ZrO<sub>2</sub> content to 15 % led to agglomeration of ZrO<sub>2</sub> particles. Furthermore, tensile results demonstrated that Al-Mg<sub>2</sub>Si composite with 10% ZrO<sub>2</sub> addition demonstrated the highest Ultimate Tensile Strength, UTS (75.35 MPa) and elongation, El % (0.69 %) compared to other fabricated composites. Hybrid composite fracture surface with 10% ZrO<sub>2</sub> revealed a more ductile fracture mode compared to other fabricated composites. This study can be beneficial to tailor new composites with refine structure and high mechanical properties.

**Keywords:** Al hybrid MMC, Mg<sub>2</sub>Si, ZrO<sub>2</sub>, microstructure, tensile properties

---

### Article Info

Received 27<sup>th</sup> October 2023

Accepted 13<sup>th</sup> December 2023

Published 20<sup>th</sup> December 2023

Copyright Malaysian Journal of Microscopy (2023). All rights reserved.

ISSN: 1823-7010, eISSN: 2600-7444

## Introduction

Magnesium silicide ( $Mg_2Si$ ) is one the most important reinforcing particles for in-situ Al matrix composites. Al- $Mg_2Si$  composites can be used for brake disks and some engine parts in automotive diligences due to their distinctive features including low density, high hardness, good strength in high-temperature, and ease of production (because the particles are added in-situ into the melt) [1]. However, low-temperature brittleness and insufficient friction properties are among their drawbacks.

Recently, the production of hybrid metal matrix composites (HMMC) is has been investigated widely. With the composition of two reinforcements in the matrix, a hybrid composite with the features of these reinforcements is produced. Hence, for composites including single reinforcement, HMMCs are good options. In applications where wear properties is crucial, these composites are utilised. Examples of frequently used reinforcements in ex-situ aluminium metal matrix composites include  $Al_2O_3$ , SiC,  $ZrO_2$ ,  $B_4C$ ,  $TiB_2$ , TiC, MgO, and  $TiO_2$  [2]. With the addition of these ceramic (reinforcements) particles to the Al- $Mg_2Si$  composite, the size of primary  $Mg_2Si$  particles is decreased, which reduces its brittleness and hardness, improving the wear and friction properties of the fabricated composite.

According to [3], nanosized SiC particulates and in-situ  $Mg_2Si$  particles reinforcing the Al-Cu matrix were used to fabricate the hybrid composites, and the microstructure and mechanical properties were investigated. The researchers showed that the mixing of in-situ  $Mg_2Si$  and ex-situ SiC can effectively alter the morphology of the  $Mg_2Si$  particles by changing them from a short strip to a dot shape as well as decreasing the average size of primary  $Mg_2Si$  particles. This results in the enhancement of the mechanical properties of the composite. Another study [4] was focused on comparing the characteristics of ADC-12 (AA383) reinforced with nano-SiC and nano- $Al_2O_3$  composites fabricated by the stir-casting method. It was found that the addition of nano-SiC and nano- $Al_2O_3$  improved the hardness value while decreasing the wear rate. An examination of the metallography and bulk hardness of artificially aged Al6061- $B_4C$ -SiC hybrid composites was conducted by Sharma et al. [5]. Compared to the aluminium alloy, considerable enhancements in tensile strength and hardness, and a minimal decrease in the ductility of hybrid composites were detected. Ghandvar et al. [6] found that the mean size of primary  $Mg_2Si$  in Al- $Mg_2Si$  composite was  $47\mu m$ , in which with the addition of 5%  $B_4C$ , the particle size decreased to  $33\mu m$ . The highest UTS (217 MPa) and El% (7%) was achieved in Al-20% $Mg_2Si$ -5% $B_4C$  hybrid composite. In another study [7] they reported that with the introduction of YSZ particles, the average size of the primary  $Mg_2Si$  particles in the base composite was  $137.78\mu m$ , which was reduced to  $88.36\mu m$  after adding 9% YSZ. The aspect ratio of  $Mg_2Si$  particles also decreased from 3, for the base composite to 1.27 in the composite containing 9% YSZ. Moreover, the hardness value displays an incremental trend from 102.72 HV, as recorded for the base in situ composite, to 126.44 HV in the composite with 9% YSZ.

A non-homogeneous distribution, weak wettability, and particles clustering in the composite matrix are the most disparaging matters faced in AMCs production. These disadvantages negatively impact the tensile properties of the composite. A few investigations of HMMCs containing  $Mg_2Si$  and  $ZrO_2$  particles were performed by [8-9]. Therefore, in this study, the impact of different contents of  $ZrO_2$  particles on microstructural and tensile properties of Al-20% $Mg_2Si$  was examined.

## Materials and Methods

In order to fabricate the ingot of the Al-20%Mg<sub>2</sub>Si composite, ADC12 alloy in commercial grade (> 98.0% purity) as well as pure aluminium (> 98.0% purity) were employed. To produce an Al-Mg<sub>2</sub>Si-ZrO<sub>2</sub> hybrid composite, initially, the ZrO<sub>2</sub> particles (> 99% purity) with a size of 10-30 μm were oxidised at 800 °C for 2 h to achieve a proper wettability with the matrix by removing the moisture and oxide layers on the surface of the particles. The contents of the ZrO<sub>2</sub> particles were fixed at 0, 5, 10 and 15%, respectively. Next, inside a graphite crucible, about 300 g of Al-20%Mg<sub>2</sub>Si composite was melted. Afterwards, the pre-oxidised ZrO<sub>2</sub> particles were added to the Al-Mg-Si melt using a stirring action at 750 °C. Then, the molten composite was held for 15 min and then heated to 720 °C and poured inside a steel die to fabricate the 30 mm thickness cylindrical samples.

Parallel to the casting of the samples, thermal analysis was conducted using a ceramic mould which was pre-heated at 500 °C for about 15 min. Around 100 g of molten composite was poured in the ceramic mould. A thermal analysis setup (EPAD-TH8-K) was used to record the temperature-time data connected to a computer with DEWESOFT software version 7.5 with a 100 Hz/ch dynamic rate. FlexPro software version 10 was used for flattening of the curves and plotting the cooling curves. The solidified rods were used to prepare the flat tensile bars based on ASTM E8/E8M. A tensile testing machine (Instron Universal 5982) set with a strain gauge extensometer was employed for conducting the tensile tests at 1.0 mm/min constant crosshead speed at room temperature. The tensile samples geometry is depicted in Figure. 1.

In order to observe the Mg<sub>2</sub>Si features in the composites, the metallographic specimens underwent the standard grinding and polishing before observing Mg<sub>2</sub>Si features in the composites using routines and were inspected using SEM. SEM (model: Philips XL40) was used to examine the specimen's microstructure characteristics, whereas the Mg<sub>2</sub>Si particles sizes were examined using the i-Solution image analyser software as a quantitative analysis system. X-ray diffraction (XRD) (PHILIPS binary diffractometer) was used for analysing the phase constituents. The SEM micrograph of the used ZrO<sub>2</sub> powders to fabricate hybrid composites with the corresponding XRD results of the particles is illustrated in Figure 2.

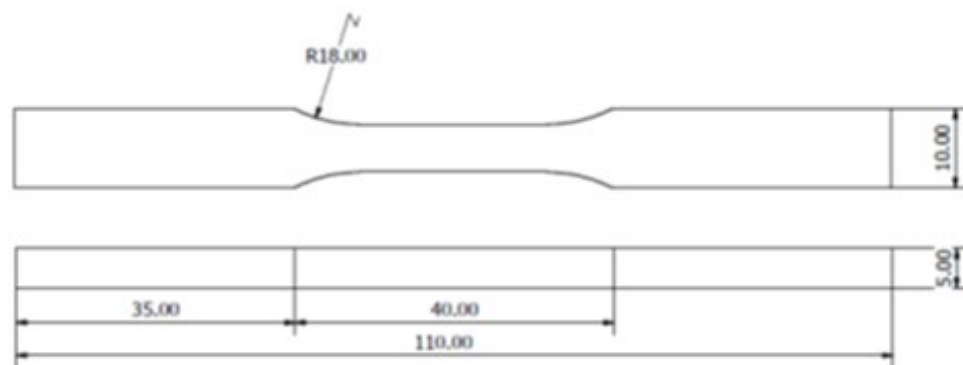


**Figure 1:** Schematic drawing of the tensile sample according to ASTM E8/E8M (all dimensions are in mm)

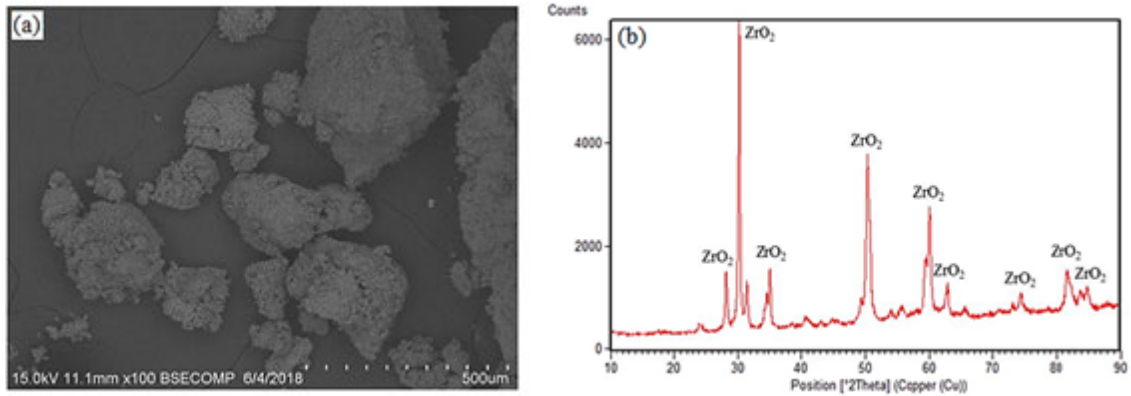


**Figure 2:** (a) SEM micrograph of  $ZrO_2$  powder and (b) corresponding XRD analysis

## Results and Discussion

### Thermal Analysis

The cooling curves and derivative curves of Al-20%Mg<sub>2</sub>Si in-situ composite with and without various concentrations of  $ZrO_2$  particles are demonstrated in Figure 3(a) to (d).

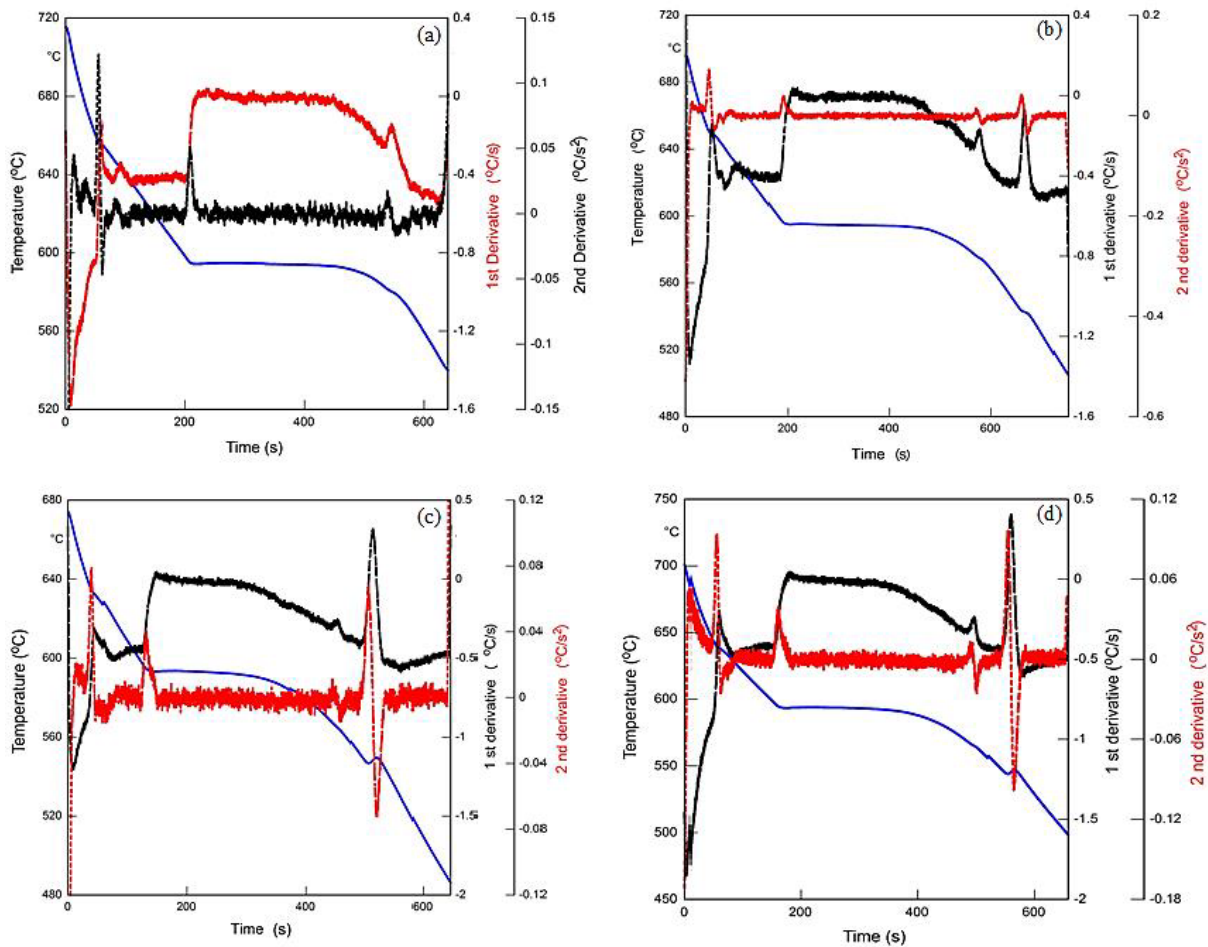


**Figure 3:** Cooling curve and related derivative curves of (a) Al-20%  $Mg_2Si$ , (b) Al/ ( $Mg_2Si+5\%ZrO_2$ ), (c) Al/ ( $Mg_2Si+10\% ZrO_2$ ) and (d) Al/ ( $Mg_2Si+15\% ZrO_2$ )

As shown, the nucleation temperature ( $T_N$ ) of primary  $Mg_2Si$  particles changed due to the influence of  $ZrO_2$  particles addition on the solidification behavior of the composite. As shown in Figure 3(a), the nucleation temperature ( $T_N$ ) of the Al-20% $Mg_2Si$  was 656.7 °C. With the introduction of 5 and 10%  $ZrO_2$ , the  $T_N$  of  $Mg_2Si$  were reduced to 650.7 and 634.4 °C, respectively. However, increasing the content of  $ZrO_2$  to 15% resulted in increasing nucleation temperature ( $T_N$ ) to 639.6 °C. This behaviour is due to the shifting of the phase diagrams (eutectic points) as a result of the addition of reinforcements [10].

### Microstructural Characterization

The micrographs of Al-20% $Mg_2Si$  composite with and without different concentrations of  $ZrO_2$  particles are illustrated in Figure 4(a) to (d). As observed in Figure 4(a), the primary  $Mg_2Si$  particle's size in the Al-20% $Mg_2Si$  composite was 50  $\mu m$ . With the addition of 5, 10, and 15%  $ZrO_2$ , the particles size of primary  $Mg_2Si$  decreased to 40, 33, and 25  $\mu m$ , respectively. In addition, with the addition of  $ZrO_2$  particles up to 10% to Al-20% $Mg_2Si$  composite, the distribution of  $ZrO_2$  particles was uniform, as presented in Figure 4. However, increasing the percentage of  $ZrO_2$  to 15% leads to non-uniformed distribution and agglomeration of  $ZrO_2$  in the Al matrix, as observed in Figure 4(d). The magnified BSE micrographs and XRD result of Al-20% $Mg_2Si$ -15% $ZrO_2$  hybrid composite are depicted in Figures 5(a) and (b), respectively, an indicative of the existence of Al as matrix and  $Mg_2Si$  and  $ZrO_2$  as reinforcement particles in the fabricated composites.

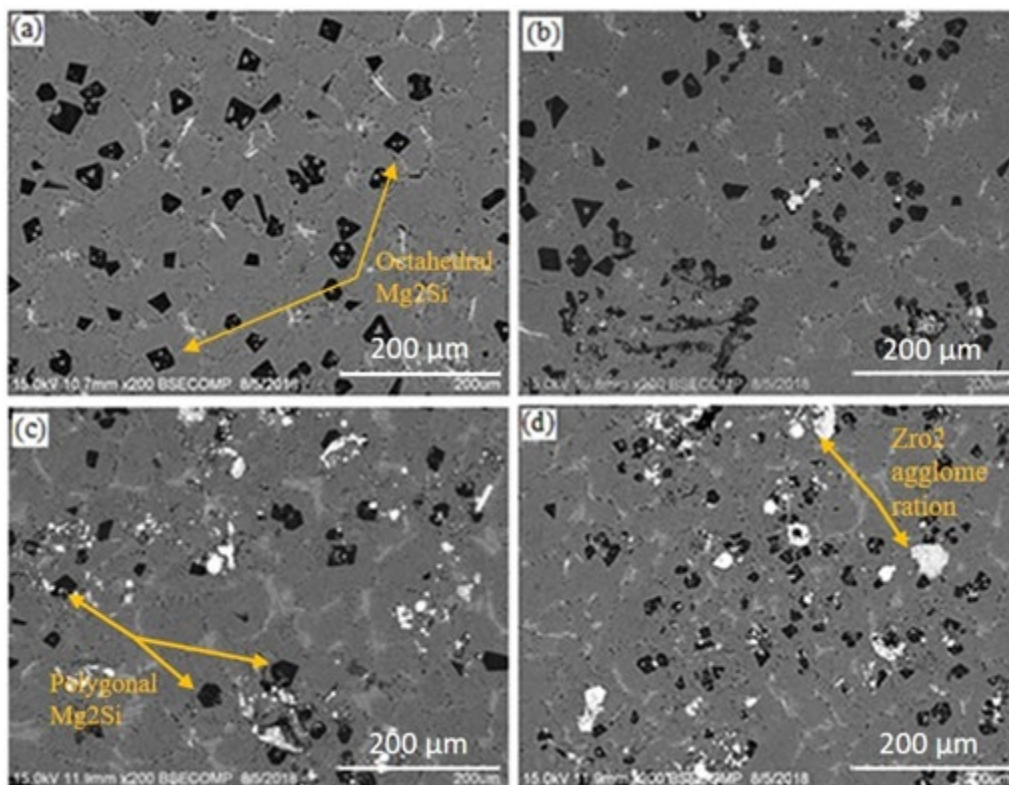


**Figure 4:** BSE electron micrographs of (a) Al-20% $Mg_2Si$ , (b) Al-20% $Mg_2Si$ -5% $ZrO_2$ , (c) Al-20% $Mg_2Si$ -10% $ZrO_2$  and (d) Al-20% $Mg_2Si$ -15% $ZrO_2$  hybrid composites



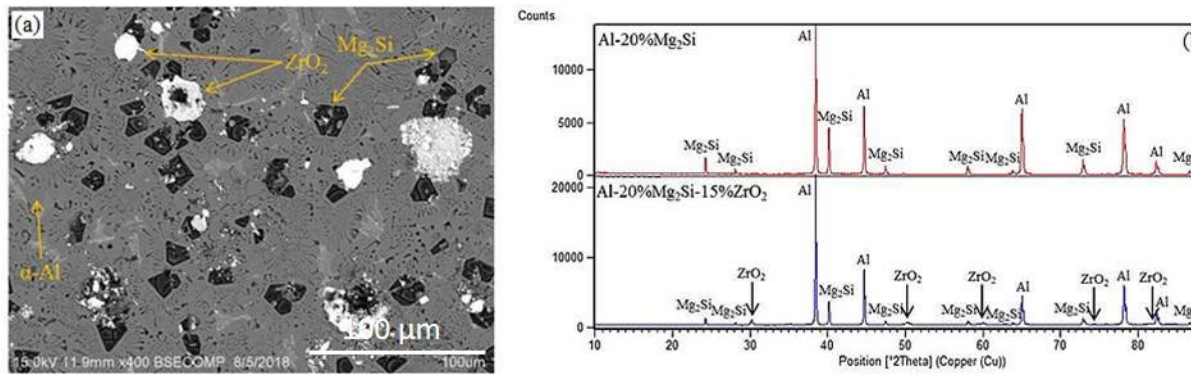


**Figure 5:** (a) BSE micrograph of Al/(Mg<sub>2</sub>Si + 15% ZrO<sub>2</sub>) and (b) Al-20%Mg<sub>2</sub>Si composites and X-ray diffraction (XRD) patterns with and without 15% ZrO<sub>2</sub> addition

### Tensile Properties

The UTS and El % of Al-20%Mg<sub>2</sub>Si composite with and without different contents of ZrO<sub>2</sub> particles are depicted in Figure 6. The UTS and El% increased by 11.7 and 22.8%, respectively with the addition of ZrO<sub>2</sub> particles up to 10%. This was due to the effect of ZrO<sub>2</sub> particles in the reduction of the primary Mg<sub>2</sub>Si particles size to 33 μm as well as the morphology alteration of the Mg<sub>2</sub>Si crystals to polygonal shape.

Furthermore, another reason for the improvement of tensile properties of Al-Mg<sub>2</sub>Si+5/10%ZrO<sub>2</sub> is the existence of proper interfacial bounding in the MMC structure. Indeed, the applied load was supposed to be supported by ZrO<sub>2</sub> particles in the matrix through the mechanism of strengthening. The composite was supported by this mechanism by conveying the applied load from the matrix to the ZrO<sub>2</sub> particles over their interface. Therefore, in order to transfer the load effectively, a proper matrix/particles interface is needed [11]. Nevertheless, when the percentage of ZrO<sub>2</sub> exceeded 15%, the tensile properties (UTS and El (%)) decreased due to the agglomeration of ZrO<sub>2</sub> reinforcement in the Al matrix.

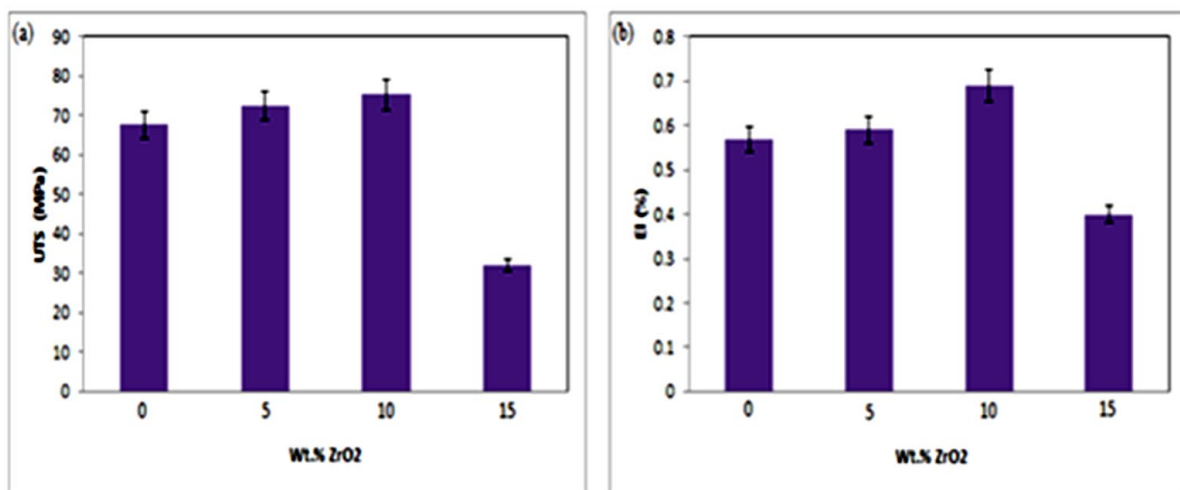


**Figure 6:** (a) UTS and (b) El% of Al-20%Mg<sub>2</sub>Si composite with and without different concentrations of ZrO<sub>2</sub> particles

Figures 7(a) to (h) illustrates the SEM micrographs of MMCs fracture surfaces after conducting tensile tests with 0, 5, 10, and 15% ZrO<sub>2</sub> additions in low (left) and high (right) magnifications. The cellular surface of the Al-20%Mg<sub>2</sub>Si composite as a result of fracture planes of coarse Mg<sub>2</sub>Si particles [12] is shown in Figures 7(a) and (b). In fact, cellular surface indicates the features of both brittle and ductile fractures on the fracture surface, simultaneously.

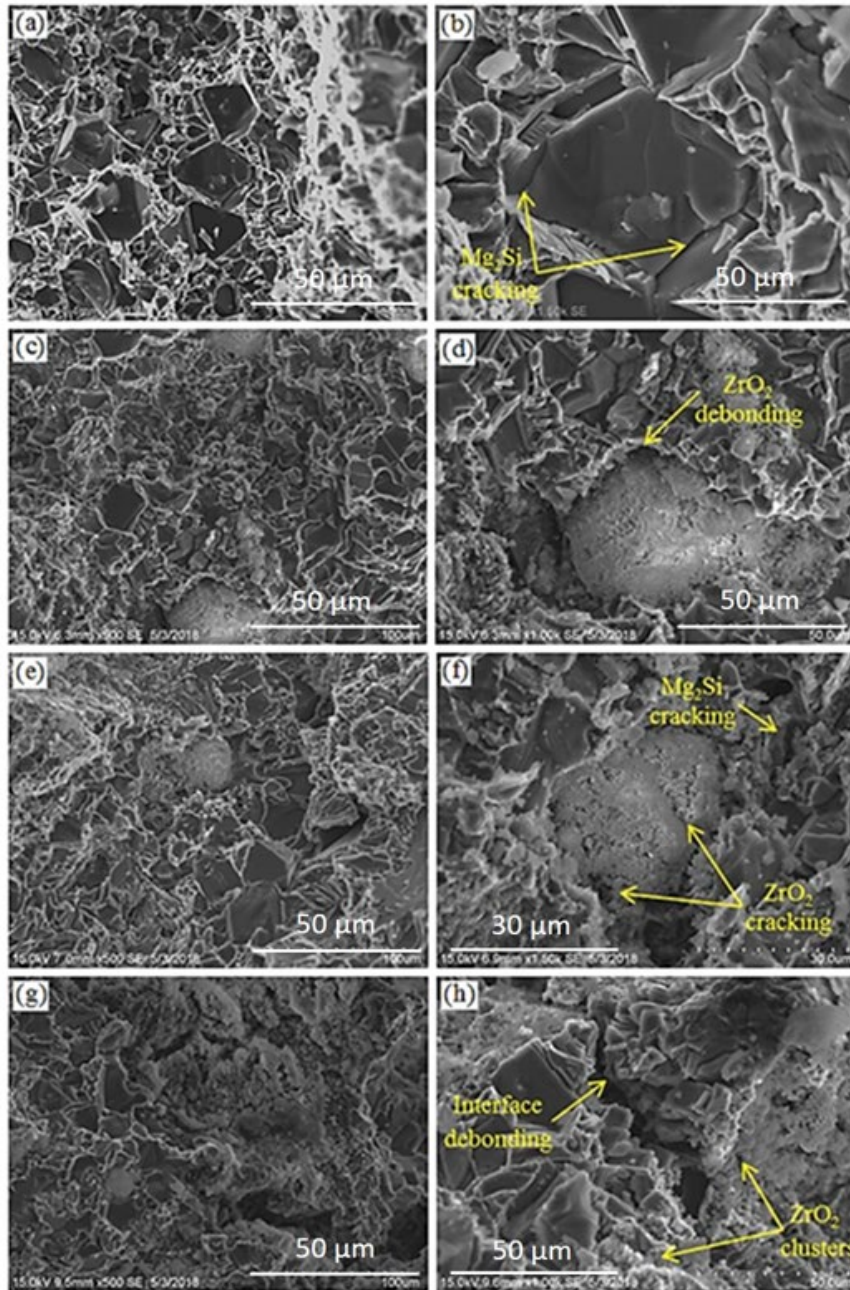


**Figure 7:** Fracture of hybrid composites with various ZrO<sub>2</sub> concentrations. (a,b) 0, (c,d) 5, (e,f) 10, and (g,h) 15% in low (left) and high (right) magnifications.

The fracture faces of almost all coarse Mg<sub>2</sub>Si particles exhibit clear cleavage characteristic creating a rapid fracture deriving from their intrinsic brittleness and pre-cracked structure [13]. As observed in Figure 7(b), the particle fracturing took place in the Mg<sub>2</sub>Si. In

fact, in the in-situ composites, the sharp corners of coarse dendritic  $Mg_2Si$  particles were the area for localisation of stress concentration; thus, a severe crack with an acute length occurred, causing a brittle mode of fracture. Figures 7(c) and (d) illustrate the Al- $Mg_2Si$ +5% $ZrO_2$  fracture surface. As shown in Figure 7(d), debonding can be observed in the particle/matrix interface. In fact, the localisation of the stress at the particles' sharp corners may also results in the debonding between the matrix and particles, a likely source of the composite failure.

The Al-20% $Mg_2Si$ -10% $ZrO_2$  fracture surface is exhibited in Figures 7(e) and (f). As observed, particle cracking was detected on the fracture surface which designated a strong bonding in the matrix/particle interface, indicative of ductile fracture mode. Therefore, stretching load application would result in better support by the  $ZrO_2$  particles. Nevertheless, the fracture surface of Al/ ( $Mg_2Si$ +15%  $ZrO_2$ ) in Figures 7(g) and (h) exhibited a clear cleavage on the hybrid composite fracture surface, a result of inappropriate wettability between matrix and  $ZrO_2$ . Thus, clustering of the  $ZrO_2$  particles took place, representing the debonding in the particles/matrix interface (Figure 7(h)).

## Conclusions

With the introduction of the  $ZrO_2$  particles to molten Al-Mg-Si, Al- $Mg_2Si$ - $ZrO_2$  hybrid composite with relatively homogeneous dispersion of the  $Mg_2Si$  and  $ZrO_2$  reinforcements was achieved through in-situ formation of the  $Mg_2Si$  particles joined with  $ZrO_2$  ex-situ technique. The addition of  $ZrO_2$  into the Al- $Mg_2Si$  composite decreased the primary  $Mg_2Si$  mean size from 50  $\mu m$  in the base composite to 25  $\mu m$  after addition of 15% $ZrO_2$ . Compared to the Al- $Mg_2Si$  composite, Al- $Mg_2Si$ -10%  $ZrO_2$  depicted the highest tensile features in terms of UTS and El (%); nevertheless, Al- $Mg_2Si$ -15%  $ZrO_2$  demonstrated low tensile properties due to the presence of porosity and  $ZrO_2$  agglomeration in the fabricated composites. Cracking of the particles was detected on the fracture surface of the Al/ ( $Mg_2Si$ +10%  $ZrO_2$ ) hybrid composite, indicating more ductile fracture.

## Acknowledgements

This work is funded by the Ministry of Higher Education under the Fundamental Research Grant Scheme (FRGS), Registration Proposal No: FRGS/1/2022/TK10/UTM/02/45.

## Author Contributions

All authors contributed toward data analysis, drafting and critically revising the paper and agree to be accountable for all aspects of the work.

## Disclosure of Conflict of Interest

The authors have no disclosures to declare.



## Compliance with Ethical Standards

The work is compliant with ethical standards.

## References

- [1] Kaushik, N. C. & Rao, R. N. (2016). The Effect of Wear Parameters and Heat Treatment on Two Body Abrasive Wear of Al–SiC–Gr Hybrid Composites. *Tribology International*. 96, 184.
- [2] Ghandvar, H., Farahany, S., Idris, M. H. & Daroonparvar, M. (2015). Dry Sliding Wear Behavior of A356-ZrO<sub>2</sub> Metal Matrix Composite. *Advanced Materials Research*. 1125, 116-120.
- [3] Li, J., Zhao, G., Wu, S., Huang, Z., Lü, S., Chen, Q. & Li, F. (2019). Preparation of Hybrid Particulates SiCp and Mg<sub>2</sub>Si Reinforced Al-Cu Matrix Composites. *Materials Science and Engineering A*. 751, 107–114.
- [4] Umanath, K., Selvamani, S. T. & Palanikumar, K. (2011). Friction and Wear Behaviour of Al6061 Alloy (SiCp+ Al<sub>2</sub>O<sub>3</sub>) Hybrid Composites. *International Journal of Engineering Science and Technology*. 3, 5441–5451.
- [5] Sharma, S. S., Jagannath, K., Prabhu, P. R., Gowri, S., Harisha, S. R. & Kini, U. A. (2017). Metallography & Bulk Hardness of Artificially Aged Al6061-B<sub>4</sub>C-sic Stir Cast Hybrid Composites. *Materials Science Forum*. 880, 140–143.
- [6] Ghandvar, H., Jabbar, M. A., Koloor, S. S. R., Petru, M., Bahador, A., Bakar, T. A. A. & Kondoh, K. (2021). Role B<sub>4</sub>C Addition on Microstructure, Mechanical, and Wear Characteristics of Al 20%Mg<sub>2</sub>Si hybrid Metal Matrix Composite. *Applied Sciences*. 11, 3047.
- [7] Ghandvar, H., Jabbar, M. A., Petru, M., Abu Bakar, T. A., Ler, L. J. & Rahimian Koloor, S. S. (2023). Role of YSZ Particles on Microstructural, Wear, and Corrosion Behavior of Al-15%Mg<sub>2</sub>Si Hybrid Composite for Marine Applications. *Journal of Marine Science and Engineering*. 11, 1050.
- [8] Yuguang, Z., Xiaobo, L., Yuanyuan, Y. & Tianjun, B. (2014). Effect of SiC Particle Addition on Microstructure of Mg<sub>2</sub>Si/Al Composite. *China Foundry*. 11(2), 91-96.
- [9] Ikeno, S., Matsuda, K., Rengakuji, S. & Uetani, Y. (2001). Precipitation Sequence in a SiC/Al-Mg<sub>2</sub>Si Alloy Composite Material. *Journal of Materials Science*. 36, 1921.
- [10] Daoud, A. & Abo-Elkhar M. (2002). Influence of Al<sub>2</sub>O<sub>3</sub> or ZrO<sub>2</sub> Particulate Addition on the Microstructure Aspects of AlNi and AlSi Alloys. *Journal of Materials Processing Technology*. 120, 296–302.
- [11] Chawla, N. & Shen, Y. (2001). Mechanical Behavior of Particle Reinforced Metal Matrix Composites. *Advanced Engineering Materials*. 3, 357-370.

[12] Lewandowski, J. J., Liu, C. & Hunt Jr, W. H. (1989). Effects of Matrix Microstructure and Particle Distribution on Fracture of An Aluminum Metal Matrix Composite. *Materials Science and Engineering A*. 107, 241–255.

[13] Warmuzek, M. (2004). *Aluminium Silicon Casting Alloys: An Atlas of Microfractographs*. (ASM International), pp. 1-124.